



## *In situ* deposition of platinum nanoparticles on bacterial cellulose membranes and evaluation of PEM fuel cell performance

Jiazhi Yang<sup>a</sup>, Dongping Sun<sup>a,\*</sup>, Jun Li<sup>a</sup>, Xujie Yang<sup>a</sup>, Junwei Yu<sup>a</sup>, Qingli Hao<sup>a</sup>, Wenming Liu<sup>b</sup>, Jianguo Liu<sup>b,\*</sup>, Zhigang Zou<sup>b</sup>, Jun Gu<sup>b</sup>

<sup>a</sup> School of Chemistry and Chemical Engineering, Nanjing University of Science and Technology, Nanjing 210094, PR China

<sup>b</sup> Eco-materials and Renewable Energy Research Center, Department of Materials Science and Engineering and National Laboratory of Solid State Microstructures, Nanjing University, Nanjing 210093, PR China

### ARTICLE INFO

#### Article history:

Received 23 September 2008

Received in revised form 20 May 2009

Accepted 24 May 2009

Available online 6 June 2009

#### Keywords:

Bacterial cellulose

Platinum nanoparticles

Membrane electrode assembly

Cyclic voltammetry

Proton exchange membrane

### ABSTRACT

*In situ* deposition of platinum (Pt) nanoparticles on bacterial cellulose membranes (BC) for a fuel cell application was studied. The platinum/bacterial cellulose (Pt/BC) membranes under different experimental conditions were characterized by using SEM (scanning electron microscopy), TEM (transmission electron microscopy), EDS (energy dispersive spectroscopy), XRD (X-ray diffractometry) and TG (thermo-gravimetric analysis) techniques. TEM images and XRD patterns both lead to the observation of spherical metallic platinum nanoparticles with mean diameter of 3–4 nm well impregnated into the BC fibrils. TG curves revealed these Pt/BC composite materials had the high thermal stability. The electroadsorption of hydrogen was investigated by CV (cyclic voltammetry). It was found that Pt/BC catalysts have high electrocatalytic activity in the hydrogen oxidation reaction. The single cell performance of Pt/BC was tested at 20 °C, 30 °C, and 40 °C under non-humidified conditions. Preliminary tests on a single cell indicate that renewable BC is a good prospect to be explored as membrane in fuel cell field [B.R. Evans, H.M. O'Neill, V.P. Malyvanh, I. Lee, J. Woodward, Biosens. Bioelectron. 18 (2003) 917].

© 2009 Elsevier Ltd. All rights reserved.

## 1. Introduction

There is a growing interest over the past several decades in the development of proton exchange membrane fuel cells (PEMFC) due to their advantages of high power density, simplicity of operation, high energy conversion efficiency and low harmful emissions [2,3]. Proton exchange membrane (PEM), a key component of PEMFC, essentially serves for transportation of protons and prevention of fuel crossover. Up to now, perfluorinated ionomer membranes (PFIM) such as Nafion have been considered to be the predominant choice for polymer electrolyte membranes due to high proton conductivity and chemical and physical stability. However, the PFIM still have some shortcomings such as high cost, limited operation temperature and high fuel permeability strongly hindering the commercialization of fuel cells [4]. To improve the performance of PEM, considerable efforts have been devoted to modify Nafion membrane or to develop alternative new hydrocarbon-based polymer membranes [5].

Bacterial cellulose (BC), which is synthesized by *Acetobacter xylinum*, is a natural and low-cost biopolymer [6]. It has many excellent properties such as high water holding capacity,

biodegradability, and high tensile strength [7]. Meanwhile, BC membranes can retain its chemical and thermal stability up to 275 °C with high mechanical strength [8]. Furthermore, the hydroxyl groups on its backbone can provide BC with a high hydrophilicity, which is crucial for the operation of polymer electrolyte membrane fuel cells [9].

A recent study showed that BC possessed reducing groups capable of initiating the precipitation of palladium, gold, and silver from aqueous solution [1,10]. In contrast, sodium hexachloroplatinate was not reduced to platinum by the action of BC. Platinum is considered the best electrocatalyst for the four-electron reduction of oxygen to water in acidic environments as it provides the lowest overpotentials and the highest stability [11–12]. In this work platinum nanoparticles were deposited on the BC membrane surface through the *in situ* chemical-reduction method. This development of new methods of membrane electrode assemblies (MEAs) fabrication is expected to boost the commercialization of fuel cells.

## 2. Experimental

### 2.1. Preparation of BC pellicles

*A. xylinum* NUST4.2 was grown in a static culture containing 20 g/l D-glucose, 21 g/l sucrose, 10 g/l yeast extract, 4 g/l (NH<sub>4</sub>)<sub>2</sub>SO<sub>4</sub>, 2 g/l KH<sub>2</sub>PO<sub>4</sub>, and 0.4 g/l MgSO<sub>4</sub> dissolved in deionized water (DI)

\* Corresponding authors. Tel.: +86 25 84315256; fax: +86 25 83621219.

E-mail addresses: [dongpingsun@163.com](mailto:dongpingsun@163.com) (D. Sun), [jianguoliu@nju.edu.cn](mailto:jianguoliu@nju.edu.cn) (J. Liu).

at 29 °C for 7 days. The pH of the medium was adjusted to 6.0–6.2 by 2.5 M NaOH. BC pellicles were purified by soaking in DI at 70 °C for 3 h and then 1 M NaOH in DI at 70 °C for 90 min. Samples were rinsed with DI to pH 7 and stored in refrigerator at 4 °C prior to use.

## 2.2. In situ preparation of Pt/BC nanocomposite membranes

For *in situ* preparation of platinum nanoparticles in 3D network structure of BC membrane was conducted through liquid phase chemical deoxidation method. Firstly, the BC pellicles were cut into small pieces, and comminuted by high speed homogenizer. Secondly, the BC homogenates were soaked in a 5 mM solution of hexachloroplatinic acid ( $\text{H}_2\text{PtCl}_6 \cdot 6\text{H}_2\text{O}$ ) dissolved in 50 mM sodium citrate, pH 5.0 and incubated at 40 °C for 12 h, the hexachloroplatinate is not spontaneously reduced inside the cellulose. Thirdly to induce platinum nanoparticles precipitation, the soaked BC homogenates were then rinsed with DI and reduced by 1.5 M solution of  $\text{NaBH}_4$  or HCHO into the cellulose matrix at 45 °C for 24 h, under vigorous stirring, when the pellicles were completely black in appearance. This material was termed Pt/BC nanocomposite. The corresponding samples are denoted as BH-Pt/BC or HC-Pt/BC. Finally, the obtained platinum/BC composites were rinsed with DI and freeze dried.

## 2.3. Chemical modification of BC membranes

In the present study, doping with proton acid or inorganic acid on the BC pellicles was performed in an attempt to enhance the capability of proton exchange [13–14]. Modification of matrix was prepared by equilibrating dehydrated BC composites in 5% solution of  $\text{H}_3\text{PW}_{12}\text{O}_{40} \cdot 29\text{H}_2\text{O}$  (PWA), for 12 h. The modification of BC membranes was frozen at –40 °C and dried in a vacuum at –52 °C.

## 2.4. Characterization

The morphology and composition of the obtained composites were analyzed by using scanning electron microscopy (SEM, JEOLJSM-6380LV) transmission electron microscopy (JEM-2100), and energy dispersive spectroscopy (EDS, ISIS30). Thermogravimetric analysis (TG) and differential thermal analysis (DTA) were carried out by using a TGA/SDTA85 instrument. The samples were kept in a platinum crucible and heated in a furnace, flushed with air at the rate of  $200 \text{ ml min}^{-1}$ , from 30 °C to 700 °C, at a heating rate of  $10 \text{ °C min}^{-1}$ . Platinum/BC nanocomposite were crystallographically characterized by X-ray diffractometry (Bruker D8 ADVANCE) with an area detector using a Cu K $\alpha$  source ( $\lambda = 1.54056 \text{ \AA}$ ) operating at 40 kV and 40 mA.

## 2.5. Electrochemical measurements

The electrochemical characterization was carried out by the cyclic voltammetry (CV) using a potentiostat (CHI630B) connected to a three-electrode test cell. The working electrode was a thin layer of BH-Pt/BC or CH-Pt/BC cast on a piece of PTFE hydrophobized carbon paper ( $0.5 \text{ cm} \times 1.0 \text{ cm}$ ). The loading of Pt on the carbon paper was  $0.5 \text{ mg cm}^{-2}$ . Platinum plate and a saturated calomel electrode (SCE) were used as the counter and the reference electrode. The Pt surface areas of the catalysts were estimated from hydrogen adsorption charges in cathodic voltammograms, which were obtained between –0.2 V and +1.2 V versus SCE at a scan rate of 50 mV/s in N-purged electrolytes. For cyclic voltammetry of hydrogen adsorption, the electrolyte solution which is 0.5 M  $\text{H}_2\text{SO}_4$  was de-aerated with high-purity nitrogen for 2 h prior to measurement.

A single fuel cell was assembled from a MEA, two copper net plates on the supply sides for gas, and two Teflon gaskets. The construction of single fuel cell is shown in Fig. 1a. The PEM is hydrated

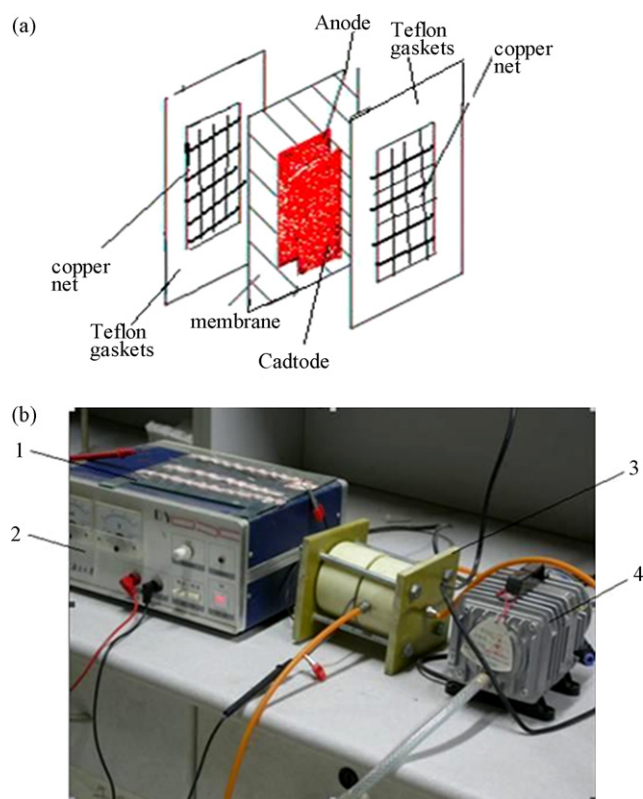


Fig. 1. The construction and testing of the fuel cell (a) the construction of single fuel cell and (b) fuel cell testing system; 1-load resistance, 2-voltage and current measurement, 3-single fuel cell, 4-air fan.

native or chemical modification of BC. The BH-Pt/BC (20 wt%) or Pt/C (E-TEK 20 wt% Pt/C) and the acetylene black (3 wt%) were ultrasonicated and stirred in the distilled water–isopropanol (1:3 volume ratio) solution for 12 h to obtain a homogeneous black suspension solution. The catalyst ink was brushed onto both sides of the membrane with the Pt loading of  $0.5 \text{ mg cm}^{-2}$ , and then this assembly was rapidly dried applying a vacuum dryer. The drying step caused the assembly to become dehydrated to MEA. The MEA may be assembled together by H-bonding between the fibrils without adhesives or glues, so the catalyst layers can prevent the bonding or the catalysts can be destroyed due to the bonding process [15]. Current generated by application of  $\text{H}_2$  to the anode of the MEA, was measured by an ammeter connected to the current collectors. The total thickness of the MEA was approximately  $100 \text{ }\mu\text{m}$  and the active area of MEA was  $6.25 \text{ cm}^2$ . The flow rate of  $\text{H}_2$  and  $\text{O}_2$  was regulated by a flow meter at 10 and  $20 \text{ cm}^3/\text{min}$ . The single fuel cell testing system is shown in Fig. 1b.

## 3. Results and discussion

### 3.1. SEM observation and EDS analysis

The SEM images of bare BC nanofibers and the TEM images of Pt/BC hybrid nanofibers are presented in Fig. 2. The SEM image of Fig. 2a shows a side view of the BC nanofibers, with an average diameter of about 30 nm and a length ranging from micrometers up to dozens of micrometers. The well-organized three-dimensional network structure is synthesized by *A. xylinum* during culture. As can be seen from Fig. 2a, the BC is porous with interconnecting pores. The pore size varies in a 5–10  $\mu\text{m}$  range. With this structure, BC own the ability to incorporate fine divided metals [16]. The TEM images of Pt/BC nanocomposite membranes show that nanoparticles are discrete in BC (Fig. 2b and c). The migration of platinum nanoparticles

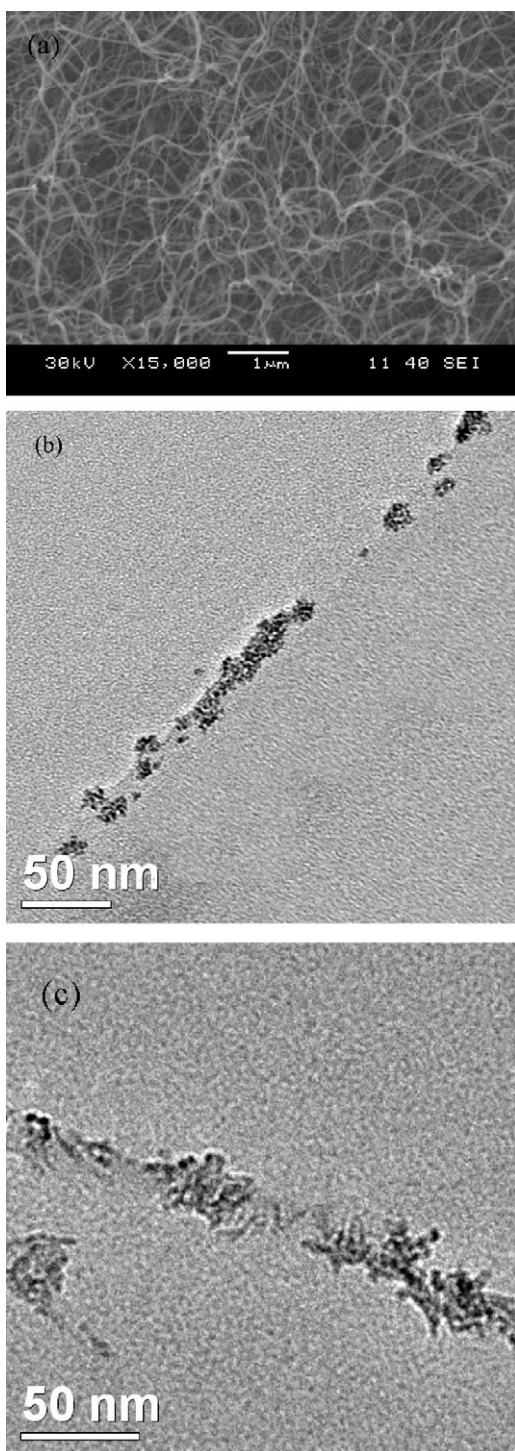


Fig. 2. SEM and TEM micrograph of: (a) BC; (b) BH-Pt/BC; (c) HC-Pt/BC.

to the inner structure of BC can be explained by a mass diffusion driven process. In fact, bacterial cellulose contains 95% of water, which in this experiment corresponds to have a porous membrane separating an aqueous colloid from bulk water. For comparison, when  $\text{NaBH}_4$  and  $\text{HCHO}$  were used to reduce  $\text{Pt}^{4+}$  to Pt metal (Reactions (1) and (2)), we found that there are some differences in platinum nanoparticles scale. The effects of the liquid phase chemical deoxidization method on the morphology of resulting platinum nanoparticles were strongly dependent on the reducibility of reductants. Typical TEM images of the BH-Pt/BC presented in Fig. 2b show remarkably more uniform and higher dispersion of the metal par-

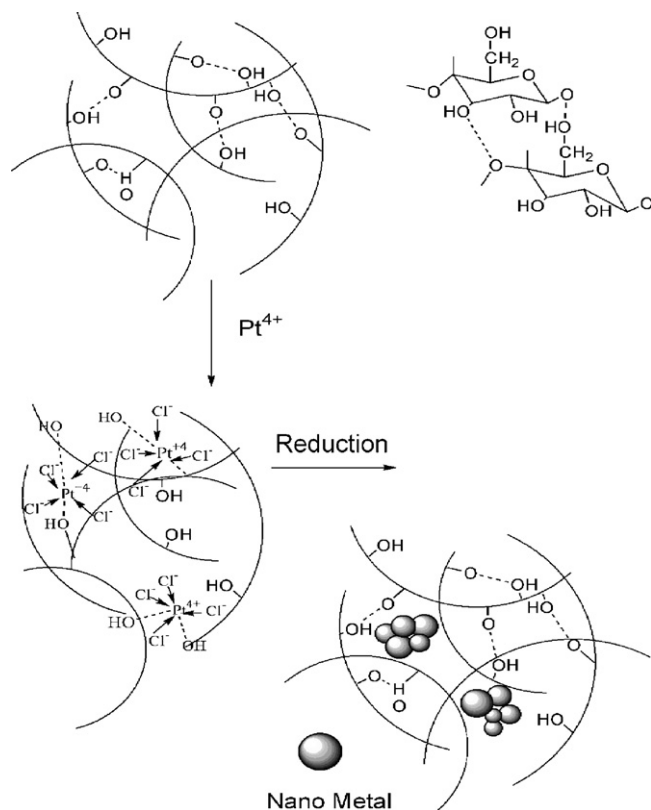
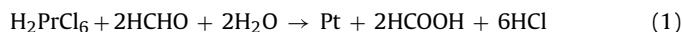


Fig. 3. Schematic illustration of the process of preparation of Pt/BC.

ticles than TEM images of the CH-Pt/BC presented in Fig. 2c. The average diameters of 3.3 nm for BH-Pt/BC and 3.9 nm for CH-Pt/BC were observed through these images.



The platinum/BC nanocomposite membranes were determined by SEM-EDS. Platinum atoms were detected on both BH-Pt/BC and CH-Pt/BC samples, confirming that through liquid phase chemical deoxidization method is an effective method of *in situ* preparation of platinum nanoparticles on the surface of BC membrane. The synthesis of the Pt catalyst imbedded in BC can be explained by the following *in situ* deposition mechanism (shown in Fig. 3). At first diffusion of Pt ions into BC matrix leads to coordination with the cellulose nonionic hydroxyl groups.  $\text{NaBH}_4$  or  $\text{HCHO}$  is then added to the solution to reduce the platinum. The average Pt contents of BH-Pt/BC samples surface is 19.2 wt% (Table 1), which is higher than the CH-Pt/BC (14.4%). The high platinum contents of BH-Pt/BC surface are possible due to reaction of *in situ* preparation of platinum in strong reducing environments faster than in weak reducing environments, the faster reaction leads to increase in the total deposited platinum on membrane surface and to lower the platinum penetration in the membrane.

Table 1  
The composition of element in the platinum/BC.

Sample	% Element					Total
	C	O	Na	Cl	Pt	
BH-Pt/BC	47.95	29.8	1.37	1.68	19.2	100.00
HC-Pt/BC	49.84	33.2	1.05	1.51	14.4	100.00

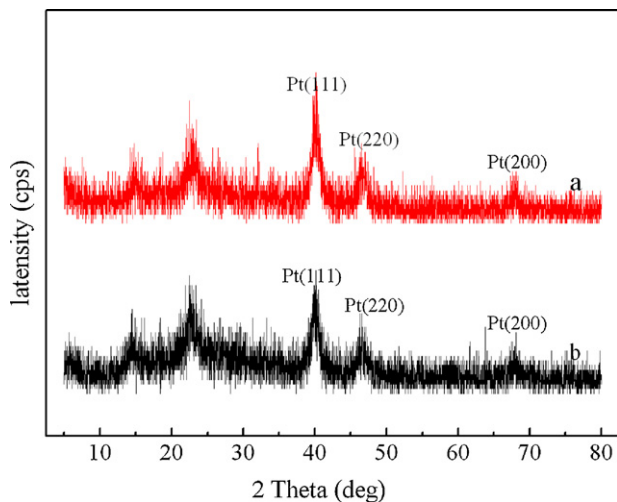


Fig. 4. X-ray diffraction patterns of samples: (a) BH-Pt/BC; (b) HC-Pt/BC.

### 3.2. XRD analysis

The XRD patterns of Pt/BC under different reductant agent conditions are given in Fig. 4. In the case of two broad peaks located at 14.6, and 23.2 are attributed to the BC. The two catalysts exhibited characteristic diffraction peaks of Pt (1 1 1) at  $2\theta$  of  $39.8^\circ$ , Pt (2 0 0) at  $2\theta$  of  $46.9^\circ$ , and Pt (2 2 0) at  $2\theta$  of  $67.5^\circ$ . The peaks can be indexed to the [1 1 1], [2 0 0], [2 2 0] reflections of a Pt face-centered cubic (fcc) crystal structure. The broader diffraction peaks for the two catalysts also lead to smaller average particle size as calculated by the Scherrer equation [17]. The calculation results, which estimated the average size of 3.1 nm for BH-Pt/BC and 3.5 nm for HC-Pt/BC, are in good agreement with the TEM measurements.

The relative contents of the Pt (1 1 1), Pt (2 0 0), and Pt (2 2 0) crystal faces can be calculated by the equation [18]:

$$I_{hkl}(\%) = \{I_{hkl}[I_{(111)} + I_{(200)} + I_{(220)}]\} \times 100 \quad (1)$$

where  $I_{hkl}$  is relative values of diffraction.

The relative content of crystal faces of the samples was shown in Table 2. XRD analysis showed that the relative content of the Pt (1 1 1) crystal face in the BH-Pt/BC is 63.1%, which is higher than the normal value of 54.35%. This benefited the acceleration of the hydrogen reaction in PEMFC [19]. The relative content of the Pt (111) crystal face in the HC-Pt/BC is 49.5%.

### 3.3. Electrochemical performances

The morphology, contents, and the relative content of the Pt (1 1 1) crystal face of the obtained platinum/BC evaluated shown that BH-Pt/BC may be more suitable for catalysts lay of fuel cell than CH-Pt/BC. So we characterized BH-Pt/BC and CH-Pt/BC catalysts electrochemically active by cyclic voltammetry in an electrolyte of 0.5 M  $H_2SO_4$  and the resulting voltammograms are shown in Fig. 5. It can be seen from Fig. 5 that the hydrogen adsorption and desorption peaks are located at about  $-0.15$  V and the Pt redox peaks are at about  $+0.5$  V. An additional anodic peak is observed at about  $0.55$  V, due to the oxidation of the surface oxide groups on the BC,

Table 2  
XRD results of platinum/BC catalysts.

Sample	$I(111)/I_0$	$I(100)/I_0$	$I(110)/I_0$
BH-Pt/BC	63.20	23.30	13.50
HC-Pt/BC	49.5	34.4	16.1
Standard value	54.35	28.80	16.85

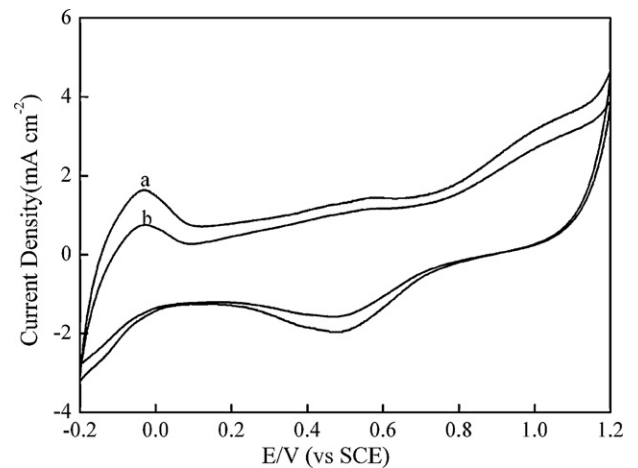


Fig. 5. Cyclic voltammograms of catalysts BH-Pt/BC and HC-Pt/BC in 0.5 M  $H_2SO_4$  at a scan rate of  $50 \text{ mV S}^{-1}$ .

in agreement with Thompson et al. [20]. It was found that the area of the hydrogen adsorption and desorption peaks for the BH-Pt/BC catalyst (Fig. 5 curve a) are much larger than that for the CH-Pt/BC catalyst (Fig. 5 curve b), indicating that the electrochemically active surface area of the BH-Pt/BC catalyst is much larger than that of the CH-Pt/BC catalyst. We measured the electrochemical specific surface area (ESA) for BH-Pt/BC and CH-Pt/BC catalysts. The surface area of ESA was calculated by using the following equation [21]:

$$EAS = \frac{Q_H}{[Pt] \times 0.21} \quad (2)$$

where [Pt] represents the platinum loading ( $\text{mg cm}^{-2}$ ) in the electrode,  $Q_H$  is the charge for hydrogen desorption ( $\text{mC cm}^{-2}$ ) and 0.21 represents the charge required to oxidize a monolayer of  $H_2$  on bright Pt [22].

The ESA of Pt are  $34.8 \text{ m}^2 \text{ g}^{-1}$  for the BH-Pt/BC catalyst and  $21.4 \text{ m}^2 \text{ g}^{-1}$  for the CH-Pt/BC catalyst. This result confirmed supposes that BH-Pt/BC may be more suitable for catalysts lay of fuel cell than CH-Pt/BC.

### 3.4. Fuel cell performance

In its normal state, a BC membrane is almost non-conductive. Although the structure of a BC monomer has several hydrogen atoms, they are strongly bonded to the structure and cannot be mobilized under the action of an electric field to make it a proton conductor. But its chemical structure can be altered to suitability for conducting proton. Doping with proton acid or inorganic acid on polybenzimidazole (PBI) has been most widely studied, and these study results show that it is a good method to increase polymer conductivity [23]. For sake of unique properties of BC, this method was used to improve BC matrix ionic conductivity and valued it by fuel cell testing system.

The polarization ( $I$ - $V$ ) characteristics of the modification BC membranes with PWA as an electrolytes, Pt/BC or Pt/C as catalysts were measured through testing fuel cell system. Figs. 6 and 7 show the several  $I$ - $V$  curves based on various MEAs in single cells at different operating temperatures. Dry hydrogen and dry oxygen gases were used as the fuel and the oxidant, respectively. These potential-current curves exhibit that, with respect to the same voltage, the current density of the cell markedly increases as the operation temperature rises from  $20$  to  $40^\circ\text{C}$ . Possible reasons may lie in the following facts. In principle, a higher operation temperature not only promotes the catalytic reactions of electrodes but also facilitates the ions to migrate through the membrane, hence, a better performance could be achieved when a relatively high operation

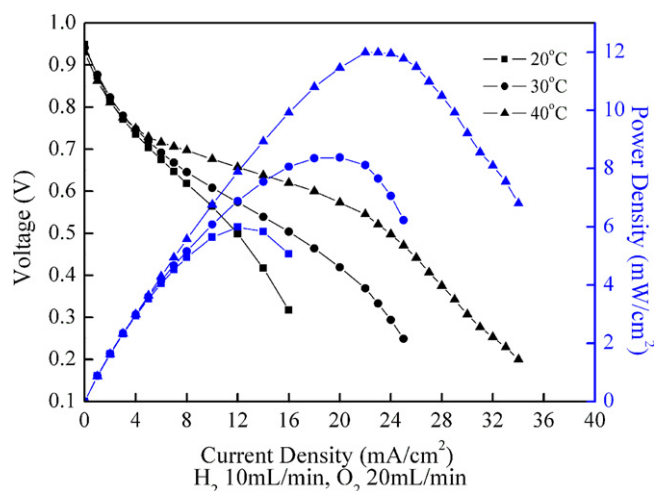


Fig. 6. Performance comparison of single cell employing the catalysts: Pt/BC with dry  $H_2/O_2$  at 20 °C; 30 °C and 40 °C.

temperature is applied [24]. Figs. 6 and 7 compare polarization characteristics of the cells with different catalysts. The maximum output of the fuel cell fabricated with the MEA on the basis of Pt/BC or Pt/C was 12.1  $mW/cm^2$ , and 19.9  $mW/cm^2$ , respectively. The obtained results show that the performance of the Pt/BC catalysts is lower in comparison with the commercialized catalyst (Pt/C). Nevertheless, the obtained results indicate that *in situ* deposition of Pt nanoparticles on bacterial cellulose is a promising way for the preparation of MEA for fuel cell applications.

### 3.5. Thermo-gravimetric analysis

Thermo-gravimetric analysis is a continuous process, involving the measurement of sample weight in accordance with increasing temperature in the form of programmed heating. We used this method to characterize membranes of BC that exhibits a weight change on heating and to detect the phase changes due to decomposition and oxidation in order to investigate thermal stability of this material. Fig. 8 shows TG–DTA curves of BC membranes measured in dry  $N_2$  from room temperature to 700 °C. Two weight-loss stages can be observed in the TG curve. At the first stage, a small weight loss of about 7% from 30 to 250 °C in TG is observed. The loss is attributed to the evaporation of loosely bound water. At the second

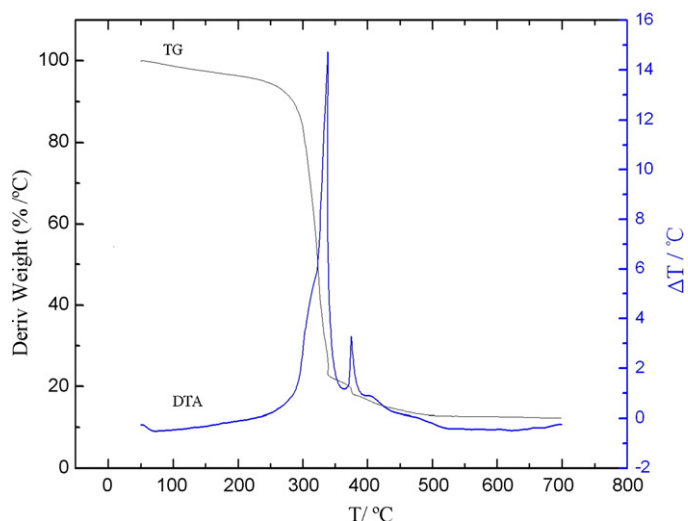


Fig. 8. Thermo-gravimetric analysis.

stage, a sharp weight loss of the membrane is observed. The significant weight loss is over 60% with an exothermic peak at around 310 °C, due to the decomposition of BC [25]. Accordingly, it may be clearly inferred that up to around 275 °C the membranes tested were found to be thermally stable, which satisfied the condition of the operating temperature 140 °C to the highest PEM hydrogen fuel cell [26]. Therefore, BC membrane is good for making PEM hydrogen fuel cells.

## 4. Conclusion

This work presents the first usage of different reduction agent to prepare Pt/BC catalyst layer through liquid phase chemical deoxidation method. The performance of this catalyst layer was tested, and the result shows it has high electrocatalytic activity. In addition, matrix proton conductivity can be improved by doping with proton acid or inorganic acid on the BC pellicles. As a result, the current density is dramatically increased. The power outputs of the cell at room temperature under non-humidified condition are obtained. Our results suggest that membranes which are renewable, thermally stable and proton-conducting, may be explored as membrane in fuel cell fields and biosensors, although there is still a lot of work to be done.

## Acknowledgments

This research is financed by Foundational Research Program of Commission of Science Technology and Industry for National Defense. The authors from Nanjing University would like to thank the support by National Basic Research Program of China (No. 2007CB613300) and Natural Science Foundation of Jiangsu Province, China (No. BK2008251).

## References

- [1] B.R. Evans, H.M. O'Neill, V.P. Malyvanh, I. Lee, J. Woodward, *Biosens. Bioelectron.* 18 (2003) 917.
- [2] S.W. Chuang, S.L. Chung, M.L. Yang, *Eur. Polym. J.* 44 (2008) 28.
- [3] C.Y. Wang, *Chem. Rev.* 104 (2004) 4727.
- [4] X.J. Cui, S.L. Zhong, H.Y. Wang, *J. Power Sources* 173 (2007) 28.
- [5] C.H. Lee, C.H. Park, Y.M. Lee, *J. Membr. Sci.* 313 (2008) 199.
- [6] D. Klemm, D. Schumann, U. Udhardt, S. Marsch, *Prog. Polym. Sci.* 26 (2001) 1561.
- [7] A. Svensson, E. Nicklasson, T. Harrah, B. Panilaitis, D.L. Kaplan, M. Britberg, P. Gatenholm, *Biomaterials* 26 (2005) 419.
- [8] J. George, K.V. Ramana, S.N. Sabapathy, J.H. Jagannath, A.S. Bawa, *Int. J. Biol. Macromol.* 37 (2005) 189.
- [9] Y. Wan, K.A.M. Creber, B. Peppley, V.T. Bui, *J. Membr. Sci.* 280 (2006) 666.

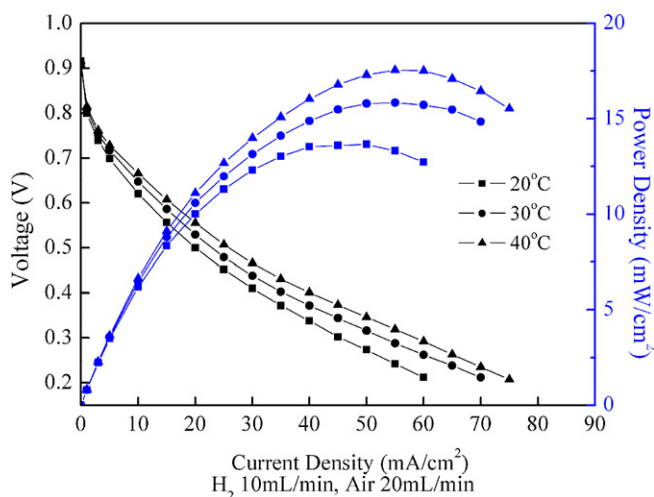


Fig. 7. Performance comparison of single cell employing the catalysts: Pt/C with dry  $H_2/O_2$  at 20 °C; 30 °C and 40 °C.

- [10] R.J.B. Pinto, P.A.A.P. Marques, M.A. Martins, C.P. Neto, T. Trindade, J. Colloid Interf. Sci. 312 (2007) 506.
- [11] H.A. Gasteiger, S.S. Kocha, B. Sompalli, F.T. Wagner, Appl. Catal. B-Environ. 56 (2005) 9.
- [12] S.C. Zignania, E. Antolini, E.R. Gonzalez, J. Power Sources 162 (2006) 105.
- [13] J. Lobato, P. Canizares, M.A. Rodrigo, J.J. Linares, J.A. Aguilar, J. Membr. Sci. 306 (2007) 47.
- [14] Y.H. Wu, C.M. Wu, F. Yu, T.W. Xu, Y.X. Fu, J. Membr. Sci. 307 (2008) 28.
- [15] P. Pfeifer, K. Schubert, G. Emig, Appl. Catal. A-Gen. 286 (2005) 175.
- [16] R.J.B. Pinto, P.A.A.P. Marques, M.A. Martins, C.P. Neto, T. Trindade, J. Colloid Interf. Sci. 312 (2007) 506.
- [17] Z.L. Liu, L.M. Gan, L. Hong, W.X. Chen, J.Y. Lee, J. Power Sources 139 (2005) 73.
- [18] J.S. Zhao, X.M. He, J.H. Tian, C.R. Wan, C.Y. Jiang, Energ. Convers. Manage. 48 (2007) 450.
- [19] J. Prabhuram, T.S. Zhao, C.W. Wang, J.W. Guo, J. Power Sources 134 (2004) 1.
- [20] S.D. Thompson, L.R. Jordan, M. Forsyth, Electrochim. Acta 46 (2001) 1657.
- [21] J.J. Wang, G.P. Yin, Y.Y. Shao, S. Zhang, Z.B. Wang, Y.Z. Gao, J. Power Sources 171 (2007) 331.
- [22] F. Maillard, M. Martin, F. Gloaguen, J.M. Leger, Electrochim. Acta 47 (2002) 3431.
- [23] H. Ye, J. Huang, J.J. Xu, N.K.A.C. Kodiweera, J.R.P. Jayakody, S.G. Greenbaum, J. Power Sources 178 (2008) 651.
- [24] Y. Wan, B. Peppley, K.A.M. Creber, V.T. Bui, E. Halliop, J. Power Sources 162 (2006) 105.
- [25] S. Gaan, G. Sun, Polym. Degrad. Stabil. 92 (2007) 968.
- [26] L. Du, S.C. Jana, J. Membr. Sci. 172 (2007) 734.